JOURNAL OF MATERIALS SCIENCE 29 (1994) 3231–3238

Nylon-6/rubber blends

Part II *Temperature effects during high speed deformation*

K. DIJKSTRA*, R. J. GAYMANS‡
University of Twente, P.O. Box 217, 7500 AE Enschede, The Netherlands

The deformation zone of fractured nylon-6/ethylene–propylene rubber specimens was studied using scanning electron microscopy (SEM). In this deformation zone three distinct layers were observed. In the main part of the stress-whitened zone only cavitation was visible. From 150–5 μm below the fracture surface, massive plastic deformation was observed. Directly under the fracture surface there was a layer about 3–5 μm thick where no cavitation or deformation was visible. This zone without cavitation was only visible when the specimen was fractured at high deformation rates. It is proposed that this top layer consists of material which was molten during fast crack propagation under adiabatic conditions. This hypothesis has been confirmed by model calculations and experiments. When the deformation rate is very high (greater than the impact velocities) plastic deformation is not homogeneous throughout the deformation zone, but confined to layers.

1. SEM studies of fractured nylon/rubber blends

1.1. Introduction

One of the striking aspects of the deformation behaviour of nylon/rubber blends is the occurrence of stress whitening in deformed samples. When fractured Izod samples are studied, stress whitening is visible in the region just ahead of the notch when the fracture type is brittle. When the specimen fails in a ductile manner, stress whitening can be seen over the entire fracture surface. Also, in unnotched dumb-bell shaped specimens, deformed in a tensile test, stress whitening can be seen over the parallel section of the gauge. Stress whitening in the unnotched samples, however, appears less intense than in the notched Izod specimens.

Stress whitening, therefore, seems to be linked to a ductile response of the blend. In the past, stress whitening in rubber-modified plastics was often associated with crazing [1, 2]. It was, however, demonstrated by Ramsteiner and Heckmann [3] that stress whitening in nylon-6,6/rubber blends could be attributed to voiding of the rubber particles. Gaymans *et al.* [4] showed that, in the neighbourhood of the crack tip of an arrested crack, the cavities became cigar shaped. A more extensive study of the stress-whitened zone of fractured nylon-6/rubber samples was performed by Speroni *et al.* [5], who showed that, also at greater distances from the fracture surface, deformed voids could be observed and that the amount of deformation was a function of the distance to the crack plane.

Recently, it has been demonstrated by Oostenbrink *et al.* [6] that the deformation zone can be divided in three layers. When approaching the fracture surface from the undeformed material, first a zone of voids (cavitated rubber particles) can be seen. Closer to the fracture surface, the number of voids grows and at a distinct point the cavities, which were round at first, become strongly deformed; now they are ellipsoid in shape. Directly under the fracture surface is a third layer where no cavitation or matrix deformation is visible. The authors suggested that local heating around the fast-running crack tip had been high enough to form a molten layer. A similar effect has been reported by Boode *et al.* [7] who found a practically undeformed layer under the fracture surface of fractured ABS Izod samples. The three-layer structure is given schematically in Fig. 1.

The work of Oostenbrink *et al.* contains two important features. First, it appears that the zone where large plastic deformation occurs is smaller than the stress-whitened zone. Second, the presence of a zone where no cavitation or deformation is visible suggests that the temperature may have risen considerably during deformation. That these thermal effects can drastically influence the mechanical behaviour during the fracture process will be clear. In the plastic zone, a rise in temperature leads to enhanced plasticity and the formation of a melt zone around the crack tip results in a reduction of the stress concentration ahead of the crack (thermal crack-tip blunting).

In order to investigate thermal effects during fracture of a nylon/rubber blend, a more quantitative analysis was made of the deformation zone of fractured Izod samples. An attempt was made to estimate the size of the plastic zone and to gain insight into the

* *Present address*: DSM Research, P.O. Box 18, 6160 MD Geleen, The Netherlands.
‡ Author to whom all correspondence should be addressed.

0022–2461

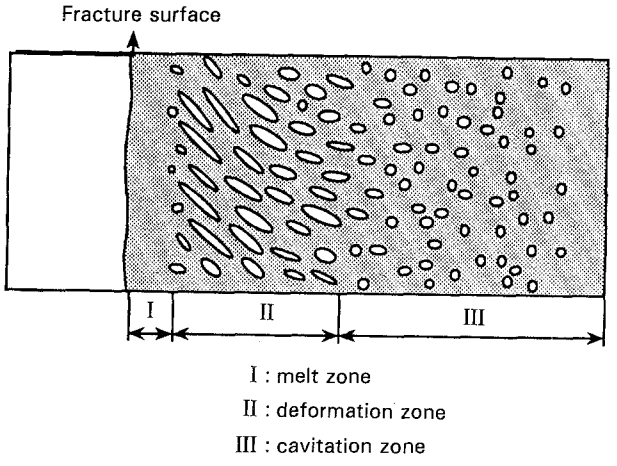

Figure 1 Schematic representation of the stress-whitened zone of a fractured nylon/rubber blend (after [6]).

amount of plastic deformation in the deformation zone.

Model studies were also carried out to examine whether it is principally possible that plastic deformation can result in melting of the material. The results of these studies are presented here.

1.2. Experimental procedure

1.2.1. Materials, blend preparation and mechanical testing

A 20 wt % nylon-6/ethylene-propylene rubber (EPR) blend was prepared by blending an injection-moulding grade nylon-6 (Akulon K124, obtained from Akzo) with an ethylene–propylene copolymer (Exxelor VA1801, kindly supplied by Exxon). Extrusion was done on a Berstorff twin-screw extruder under such extrusion conditions that a weight average particle size of 0.30 μm was obtained. The specimens (dumbbell shaped tensile specimens according to ISO R527-2 and impact specimens according to ISO 180-1A) were prepared on an Arburg Allrounder 221-55-250 injection-moulding machine. The impact specimens were fractured with a Zwick pendulum and had a notched Izod of about 60 kJ m^{-2}. Tensile tests were performed on an Instron tensile tester with a cross-head speed of 5 mm min^{-1}.

1.2.2. Sample preparation for SEM

Samples were taken from fractured Izod samples as shown in Fig. 2. The following procedure was followed. First a small beam ($l \times w \times t \approx 2.5 \times 1 \times 1.5$ mm^3) was cut out of the sample. The end which originally was in the centre of the Izod sample was trimmed carefully on three sides (excluding the fracture surface) with a fresh razor blade in such a way that a surface of 0.3×0.5 mm^2 remained. This surface was microtomed on a CryoNova LKB 2288-050 cryotome with a diamond knife. The specimen temperature during microtoming was −110 °C and the knife temperature was −100 °C. Microtoming was performed under a nitrogen atmosphere.

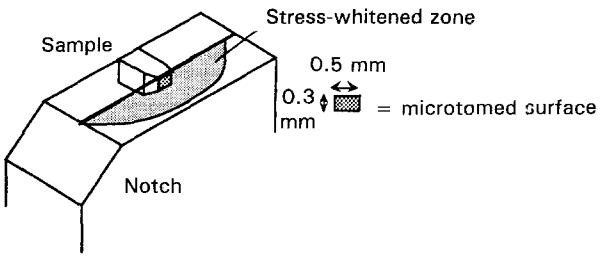

Figure 2 Position of the sample used for SEM investigations in a fractured Izod sample. The dotted area is the microtomed surface.

For studying the amount of deformation, the rubber was etched out of the surface in boiling *m*-xylene. When the objective was to study the cavitation only, the surface was cleaned in distilled water in an ultrasonic bath. Afterwards the samples were dried under vacuum at 40 °C for a few days.

1.3. Results and discussion

1.3.1. Strain distribution in the stress-whitened zone of a fractured nylon/rubber blend

Attention was first paid to the amount of deformation visible in the stress-whitened zone. Therefore, the rubber was etched out of the microtomed surface and several micrographs were taken at different depths in the deformation zone. In control experiments, presented in Part 1.3.2 of this paper, it was checked that the etching procedure (18 h in boiling *m*-xylene) did not affect the size of the deformed cavities. From these micrographs, the length and the width of the deformed cavities were determined as a function of the distance to the fracture surface. The results are given in Fig. 3 which shows that when approaching the fracture surface, the length of the cavities increases. In the same range a decrease is visible in the width of the voids, though this effect is less pronounced. It appears that the size of the zone where massive plastic deformation has taken place in this sample is only about 100 μm thick.

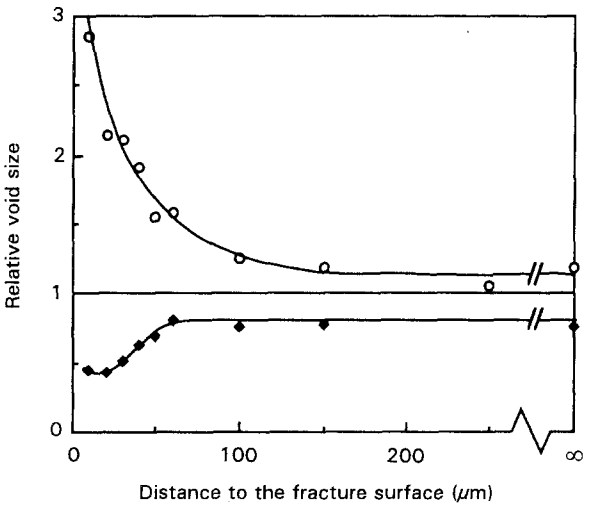

Figure 3 Void size (rubber etched out of the microtomed surface), relative to the average particle size versus the distance to the fracture surface. Sample taken from a fractured nylon-6/EPR (20 wt %) notched Izod specimen from the position as shown in Fig. 2 (○) Void length, (◆) Void width.

The thickness of the total stress-whitened zone was measured with light microscopy and was found to be 1.7 mm. This means that in only about 6% of the total stress-whitened zone, large plastic deformation has occurred.

Also in the undeformed specimens, there is a difference between the width and the length of the voids. This indicates that the particles originally were not perfectly spherical. However, no preferred orientation of the particles could be observed in samples taken from the undeformed specimens.

With the size of the deformed voids, it is possible to estimate the strain distribution in the plastic zone. When the deformation is taken to be equal to the relative length change of the void, the strain is given by

$$\varepsilon_{\text{matrix}} = \frac{l - d}{d} \quad (1)$$

where l is the length of the deformed void and d is the average particle size. The resulting strain as a function of the distance to the crack plane is given in Fig. 4. It is obvious that the strain in general is similar to the void length given in Fig. 3. The maximum strain is about 2. In the high strain region, however, the results will be less accurate because it was difficult to measure the length of the strongly deformed voids in this blend with a relatively high rubber content.

1.3.2. Matrix relaxation in the "melt" zone

As mentioned in Section 1.1, directly under the fracture surface no cavitation or matrix deformation is present. In the SEM studies reported above, no attention could be paid to this top layer because the rubber was removed from the microtomed surface. When the samples received no further treatment after the microtoming, the layer is clearly visible. In Fig. 5 a micrograph of the zone directly under the crack plane is shown and it can be seen that massive deformation starts about 3–5 μm below the fracture plane. It is also notable that the "non cavitated" layer is not totally

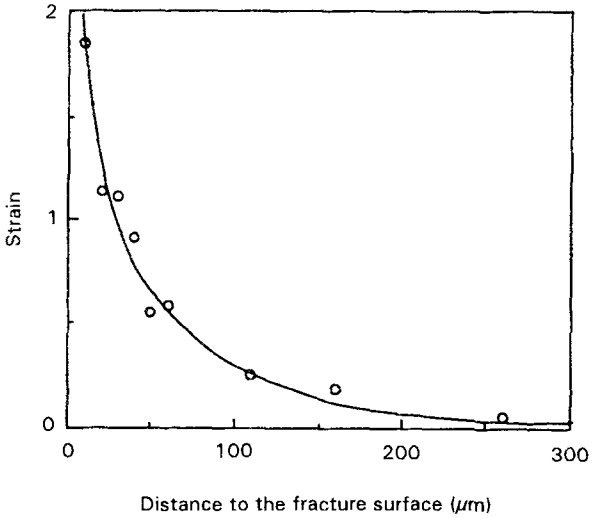

Figure 4 Estimated strain in the stress-whitened region of a fractured Izod sample. Material: Nylon-6/EPR (20 wt %, d = 0.26 μm). Strain calculated using Equation 1.

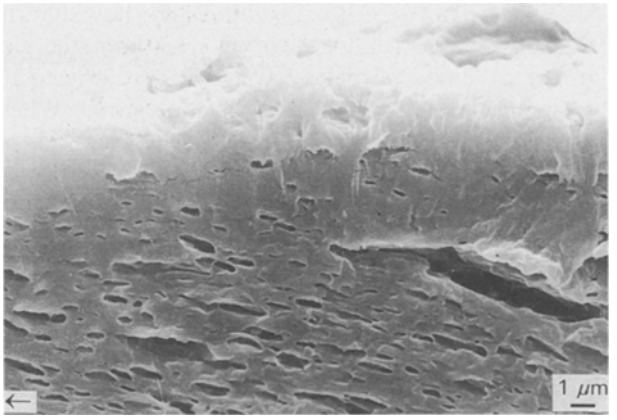

Figure 5 Scanning electron micrograph of the zone directly under the fracture surface of a fractured nylon-6/EPR blend. The rubber has not been removed from the microtomed surface. The arrow indicates the direction of crack growth (photo by A. J. Oostenbrink).

without voids, but that there is still a small number of relatively small voids.

The question of whether this layer originates from local melting, as proposed by Oostenbrink *et al.* [6], can be approached from different angles. First, if the top layer originates from a rise in temperature, at what temperature is matrix relaxation fast enough for this kind of large deformation to disappear? Second, a more theoretical approach can be followed to calculate whether it is principally possible to supply enough mechanical energy to the system to achieve this large temperature effect, given the loading time and the material parameters. The control experiments are discussed here. The calculations will be treated in Part 2.2.1 of this paper.

When dumb-bell shaped specimens are deformed up to the point of fracture and SEM studies are made of the material in the necked region and of the unnecked region, it can be seen that in the necked region, strongly deformed cavities are visible, while in the unnecked region only more or less round voids are present.

At this point we are interested in the temperature where plastic deformation and cavitation disappear. In order to study the relaxation of plastic deformation at elevated temperatures, samples were taken from the necked region. From these samples, the rubber was removed with boiling *m*-xylene. Consequently, the samples were heated in an oil bath for about 10 min; the temperature of the oil bath was varied. After the heat treatment, the samples were cleaned in an ultrasonic bath and dried at 40 °C for a few days. Micrographs were taken from these samples and the size of the cavities (i.e. the deformed particles) was measured.

When the relaxation of cavities was studied, samples were taken from the unnecked region. In this region, stress whitening is visible, but it is expected that the amount of plastic deformation is limited. These samples were not etched, which means that the voids visible on micrographs are the cavities in the rubber. The samples taken from the unnecked region received the same temperature treatment as the samples taken from the necked region. The resulting void

size is given in Fig. 6. The results clearly show that the size of the plastically deformed voids and the size of the cavitated particles have not been affected by temperatures below the melt temperature. When, however, the material has been in the melt, matrix deformation and cavitation are no longer visible in the micrographs. Therefore, it is concluded that if the observed structure of the top layer is caused by thermal effects, the local temperature rise must be high enough to melt the material.

With the length of the elongated cavities, the plastic strain in the necked region can be estimated using Equation 1. This results in a maximum strain of 2.78. The maximum strain found in a tensile experiment at low speed is therefore higher than the maximum strain achieved during impact (Fig. 4).

2. The transition from isothermal to adiabatic deformation

2.1. Introduction

It is well known that plastic deformation and rupture of polymers can be accompanied by large thermal effects. Recently, a review of thermal effects during deformation and fracture of polymers was published by Godovsky [8]. In general, there are two main sources for temperature rise in fractured polymers. Firstly, the energy dissipated during plastic deformation is partly transferred to heat. Godovsky reported, for PA-6, values for the ratio between the energy dissipated as heat and the total plastic work between 0.80 and 0.87. The remaining part of the plastic work is stored as internal energy (i.e. re-crystallisation). The second source, which is not often taken into account, is the energy released when highly stretched polymer chains are fractured.

Plastic deformation normally is accompanied by chain scission. In tests done by Godovsky *et al.* [9] it was found that just before the fracture of highly oriented nylon-6, the number of ruptured chains in nylon-6 fibres was 1×10^{19} g^{-1}. It was concluded that when a chain ruptures, the free radicals formed cause the fast fracture of tens to hundreds of adjacent stressed molecules. In this way a large number of microcracks can be formed. In SAXS measurements it was found that in the pre-ruptured state, the number of microcracks was about 5×10^{16} cm^{-3} with diameters close to 15 nm. The local adiabatic temperature rise accompanied by the formation of these microcracks was estimated to be 750 K.

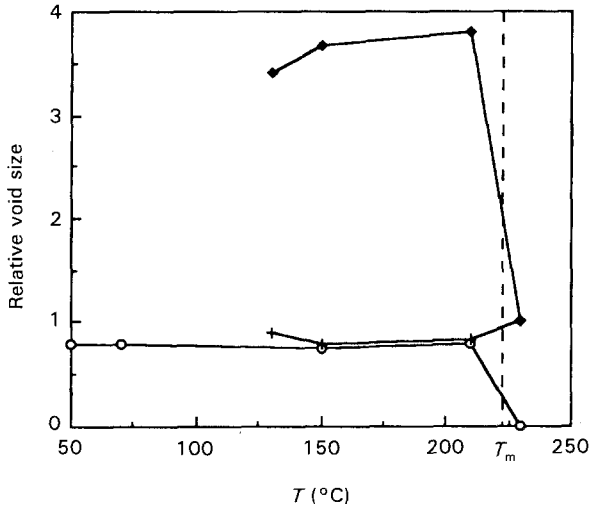

Figure 6 The void size relative to the average particle size for deformed nylon-6/EPR (10 wt %, $d = 0.42$ μm) specimens after different temperature treatments. Samples taken from the necked region (rubber etched out): (◆) size parallel to drawing direction, (+) size perpendicular to drawing direction. (○) Samples taken from the unnecked region (rubber still present). (– – –) The melt temperature of nylon-6.

When the temperature rise during deformation is studied, the adiabatic condition will not automatically hold. The maximum temperature will therefore not only be a function of the heat production (plastic work and chain rupture) but also of the strain rate, environment and specimen geometry. For cylindrical samples several authors tried to estimate theoretically the maximum temperature rise ahead of a running crack as a function of the size of the plastic zone and the crack velocity. For PMMA, values have been reported ranging from 210 K [10] up to 1200 K [11], which demonstrates that the results are strongly dependent on the model used. In the model presented by Godovsky [8], the zone where the heat is generated is approximated by a rectangular layer of thickness 2δ and length d. When the co-ordinate system is coupled with the crack tip, the problem can be treated as steady-state. The temperature profile in the heated zone is given by

$$T(x, y) = T_\infty + \frac{Q}{2\delta c_p \rho}\theta\left(\frac{x}{\delta}, \frac{y}{\delta}, \frac{d}{\delta}, \psi\right), \quad \psi = \frac{c\delta}{2a} \tag{2}$$

where Q is the heat production (J m^{-2}), c is the crack velocity and a is the heat diffusion coefficient. The velocity parameter, ψ, determines whether the deformation is isothermal or adiabatic. Godovsky showed that for $\psi < 10^{-2}$ s^{-1}, the deformation is almost isothermal, while for $\psi > 10^{1}$ s^{-1} the deformation is practically adiabatic.

2.2. Modelling of the temperature rise in nylon/rubber blends

An attempt is now made to calculate the temperature rise during deformation in nylon/rubber blends as a function of strain rate and the physical properties of the material. It is not the objective of this analysis to give an exact description of the temperature profile in the deformation zone of a blend. It was possible, though, to calculate the strain-rate regime where deformation is clearly adiabatic or isothermal.

2.2.1. The maximum temperature rise

For the calculation of the energy dissipation in the deformation zone, an assumption has to be made concerning the stress–strain behaviour in the plastic region. Fukui *et al.* [12] showed that the behaviour of nylon-6 could be well described by the behaviour of an

ideal plastic strain-hardening material. The stress–strain curve, given in Fig. 7, is given by

$$\sigma(\varepsilon) = \sigma_y + \frac{\varepsilon}{\varepsilon_b}(\sigma_b - \sigma_y) \quad (3)$$

where σ_y is the yield stress, σ_b is the fracture stress and ε_b is the fracture strain. The energy dissipation per unit of volume can be calculated simply by integrating the stress–strain curve up to the fracture strain. When it is assumed that a fraction, ϕ, of the plastic work is transformed to heat and the deformation is assumed to be purely adiabatic, the maximum temperature rise in the material is given by

$$\rho c_p \Delta T_{max} = \phi \int_0^{\varepsilon_b} \sigma(\varepsilon)\,d\varepsilon \rightarrow \Delta T_{max}$$

$$= \phi \frac{\varepsilon_b}{2\rho c_p}(\sigma_y + \sigma_b) \quad (4)$$

where ρ is the density and c_p is the heat capacity. Values for density and heat capacity of nylon-6 are readily available. The yield stress, fracture stress and fracture strain of nylon-6 have been determined by experiment. Therefore, dump-bell shaped specimens of nylon-6, type Akulon K124, obtained from Akzo, were deformed with an Instron tensile tester up to their breaking point with a draw speed of 5 mm min^{-1}. The yield stress is taken to be the engineering yield stress. The fracture stress is calculated by dividing the fracture force by the surface of the necked part of the specimen just below the fracture surface. The fracture strain follows from the ratio of surface of the necked region and the initial cross-section of the specimens. It is assumed that volume strain can be neglected (Equation 5)

$$\varepsilon_b = \frac{A_0}{A_{neck}} - 1 \quad (5)$$

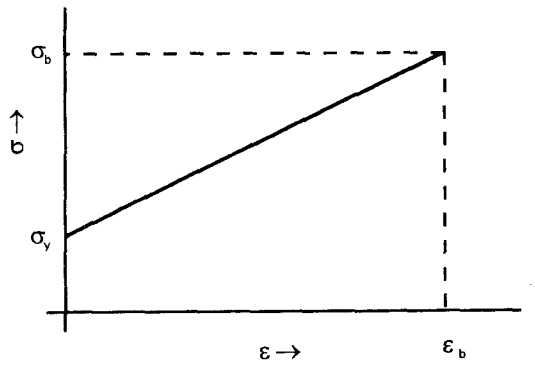

Figure 7 Idealized stress–strain curve for a plastic strain-hardening material.

For blends, the fracture strain can be calculated using the size of the deformed holes in the necked region. In this case the fracture strain can be calculated from the ratio between the length of the ellipsoid holes and the diameter of the undeformed particles. This was done for the nylon-6/EPR blends given in Fig. 6. The results are given in Table I, together with some data from the literature.

The calculations presented in Table I result in temperature rises which are considerable, but do not exceed the melting point of nylon-6. The yield and fracture stress used, however, are measured at low strain rates. With a draw speed of 1 m s^{-1} the yield stress of nylon-6 is 95 MPa [14] which would result (even if the fracture stress does not change) in an end temperature close to the melting point. The data suggest, however, that during cold drawing, insufficient energy is dissipated to melt the material.

In these results the temperature rise due to chain rupture is not included. From the results of Godovsky it follows that in the pre-ruptured state the volume fraction of microcracks is close to 0.1 (using the data given in Section 2.1). When the temperature rise of the material incorporated in the microcracks is 750 K, then the average temperature rise in the high-stressed region will be close to 70 K. This indicates that in the region of the deformation zone close to the fracture surface, where the concentration of microcracks will be high, it is in principle possible that the temperature can locally exceed the melting point.

Some attempts were made to measure the temperature rise during high-speed deformation of nylon-6, using an infrared detector. Dumb-bell shaped specimens, according to ISO R527-1 standard, were injection moulded from nylon-6 (type Akulon K124, supplied by Akzo). These specimens were deformed at a draw speed of 20 m s^{-1} (strain rate $\approx$200 s^{-1}) on a Schenck hydropuls 25 VHS high-speed hydraulic tensile tester. In these tests, macroscopic temperature rises of approximately 130 °C were measured on an arbitrary place on the specimen (spot diameter 1 mm). It might be expected that the local temperature will be higher.

2.2.2. The transition from isothermal to adiabatic deformation

When the actual heat build up in the deformation zone is considered, the flow of heat to the surroundings must also be taken into consideration. Analytical solutions for temperature distributions in non-static systems are possible only for simple configurations.

TABLE I Calculated maximal temperature rise for nylon-6. ρ = 1140 kg m^{-3}, c_p = 1600 J kg^{-1} °C^{-1}. ϕ is assumed to be 0.85.

	Nylon-6[a]	Nylon-6[b]	Nylon-6[c]	Blend[a] (10 wt % EPR)
Yield stress (MPa)	78	55		65
Fracture stress (MPa)	161	168		126
Fracture strain	2.92	1.06	3.00	2.78
ΔT_{max} (°C)	162	55		129

[a] Own data.
[b] Data taken from Fukui *et al.* [12].
[c] Data taken from Postema *et al.* [13].

Therefore, some assumptions have been made concerning the shape of the deformation zone. This deformation zone is different from the approximated rectangular deformation zone in brittle materials (Fig. 7) which was discussed in Section 2.1. With these materials, plastic deformation is limited to a small region ahead of the crack tip. In nylon/rubber blends, fracture is preceded by gross yielding of the entire cross-section of the specimen [15]. In a notched specimen, the deformation zone is, therefore, more or less planar. The following assumptions have been made:

(i) the thickness of the plastic zone is much smaller than the width and the length of the specimen. Therefore, the heat flow in the directions parallel to the fracture surface can be neglected and the problem can be treated as a one-dimensional one;

(ii) the temperature at time $t = 0$ is homogeneous;

(iii) the deformation zone is symmetrical around the fracture plane. In this way only half of the zone has to be considered. From symmetry considerations, it follows that the fracture plane is a perfectly isolating boundary (no heat flow across the future crack plane);

(iv) the deformation is homogeneous in the complete deformation zone;

(v) density, ρ, heat capacity, c_p, heat conductivity, λ, and fracture strain, ε_b, are independent of temperature, strain rate and position in the deformation zone.

The deformation process will be adiabatic if the period of time when the heat is produced, t_p, is much smaller than the time it takes for the heat to flow to the surroundings, t_f. The time, t_p, is given by a simple relation between strain rate, $\dot{\varepsilon}$, and the fracture strain

$$t_p = \frac{\varepsilon_b}{\dot{\varepsilon}} \tag{6}$$

The temperature profile in a plate with a given temperature T_0, which is perfectly isolated on one side and subjected to a temperature T_∞ on the other side, at time $t = 0$ is determined by the Fourier's number. The Fourier number, F_0, is defined as

$$F_0 = \frac{\lambda}{\rho c_p}\frac{t}{L^2} \qquad (t = t_f) \tag{7}$$

where λ is the heat conductivity, t is the time and L is the thickness of the plate. At this moment we are interested in to what extent the heat generated during plastic deformation will flow to the surroundings in the time it takes to reach the fracture strain. Therefore, $t_p = t_f$ and Equations 6 and 7 can be combined. When it is assumed that all the applied strain will be plastic ($v_d = \dot{\varepsilon} 2 r_f$, where v_d is the draw speed), Equation 8 can be derived

$$F_0 = \frac{\lambda}{\rho c_p}\frac{\varepsilon_b}{\dot{\varepsilon} r_f^2} = \frac{\lambda}{\rho c_p}\frac{2\varepsilon_b}{v_d r_f} \tag{8}$$

When $F_0 \ll 1$, the process is close to adiabatic, while for values of $F_0 \gg 1$ the process is isothermal [16]. In Table II, the Fourier number is calculated for two strain rates, similar to those applied in a tensile test, but in an impact test. It is clear that the deformation speed of an impact test results in a very low Fourier number which implicates that the deformation is almost completely adiabatic. Conversely, the draw speed of a normal tensile tests gives the Fourier number much greater than 1. In this case, the deformation will be almost isothermal. In Table II, the velocity parameter, ψ (Equation 2), is also calculated. The crack velocity, c, is taken to be the average crack velocity which can be calculated from the time it takes the crack to grow to completion and the width of the specimen. These values also indicate that increasing the draw speed from 0.1 mm s^{-1} to 1 m s^{-1} results in a transition from close to isothermal to adiabatic deformation.

The model presented here is a very simple one, suitable to estimate whether the deformation is applied under almost adiabatic, or isothermal conditions. In the transition region between the two ideal situations, the approach is no longer valid. In that case, temperature profiles can be calculated using FEM approximations.

3. Influence of strain rate on the structure of the deformation zone

Until now, the three-layer structure in the deformation zone of fractured nylon/rubber blends has only been demonstrated in specimens deformed under impact conditions where deformation is almost purely adiabatic. When the presence of an undeformed top layer directly under the fracture surface is a consequence of an adiabatic temperature rise of the material up to temperatures close to or above the melting point, it is expected that this top layer will be absent when the deformation is isothermal.

Dijkstra *et al.* [17] discussed notched tensile impact tests on nylon-6/EPR specimens with the same geometry as the Izod specimen. With this test it was possible to vary the strain rate over a broad range. From these tests samples which were fractured with varying strain rates were studied in a similar way as described in Fig. 2. It appeared that the samples deformed with a draw speed of 1 m s^{-1} (comparable to

TABLE II The Fourier number for two different test speeds. The size of the plastic zone is estimated from SEM studies of fractured samples

v_d (m s^{-1})	r_f (μm)	λ (J s^{-1} m^{-1} $°C^{-1}$)	ρ (kg m^{-3})	c_p (J kg^{-1} $°C^{-1}$)	ε_b	F_0	c (m s^{-1})	ψ (s^{-1})
0.0001	250	0.23	1140	1600	2.92	29.4	0.0002	0.42
1	100	0.23	1140	1600	2.92	0.008	3.709	2941

the deformation rate in the Izod test) had a deformation zone very similar to those found in fractured Izod samples. In Fig. 8a, an example is given of the top layer of the deformation zone of a specimen tested with a draw speed of 1 m s^{-1}.

When the same material, but now fractured with a draw speed of 0.5 mm min^{-1}, is studied, it can be seen that the matrix deformation and cavitation is now visible up to the fracture plane. This indicates that indeed the observed top layer originates from a temperature rise (Fig. 8b). Except for the absence of the undeformed top layer, the structure of the deformation zone of specimens fractured at low speed and under impact conditions (v_d = 1 m s^{-1}) are quite similar. This changes when the draw speed is increased to the highest speed possible with the equipment used (v_d = 12.5 m s^{-1}). In Fig. 9, a micrograph of the deformation zone of a specimen fractured with a draw speed of 12.5 m s^{-1} is shown. The deformation is now concentrated in thin layers of about 15 μm thick, approximately parallel with the fracture surface. A number of these zones was visible in the stress-whitened zone. At some places two different zones intersected. The structures look very similar to crazes, only they are much coarser.

There is, as yet, no solid explanation for this behaviour. Possibly, it originates from the fact that cavitation also propagates preferably in bands perpendicular to the maximum principal stress [18]. From Equation 8 it follows that with increasing test speed, the thickness of a deformation zone can decrease while the zone still is under adiabatic conditions. Plastic deformation starts in the cavitated zones. When the draw speed is high enough for these zones to deform adiabatically, deformation can be concentrated in these layers via thermal stress softening.

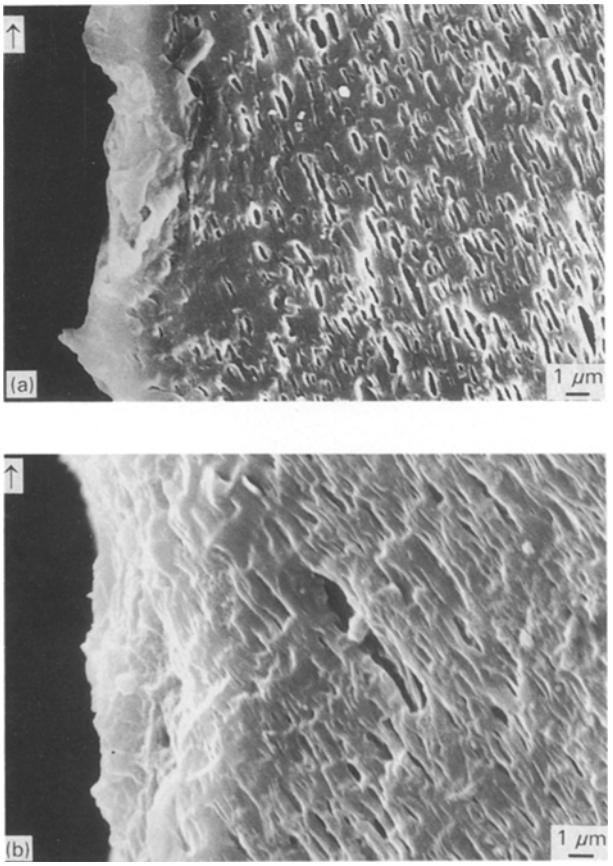

Figure 8 Fracture zone of a fractured nylon-6/EPR (20 wt %, d = 0.3 μm) blend. (a) Draw speed = 1 m s^{-1}, (b) draw speed = 0.5 mm min^{-1}. The arrow indicates the direction of crack growth.

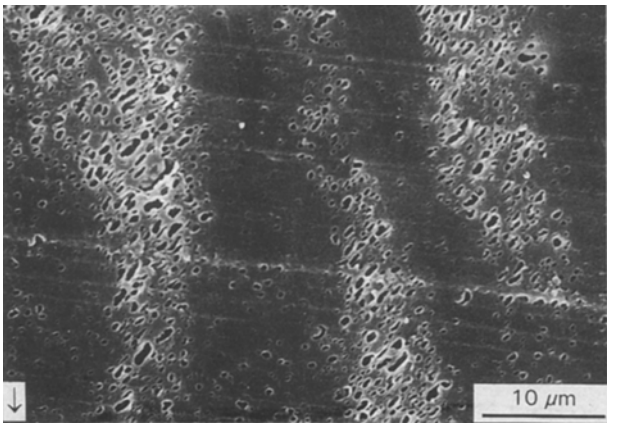

Figure 9 Fracture surface of a fractured nylon-6/EPR (20 wt %, d = 0.3 μm) blend. Draw speed = 12.5 m s^{-1}; the arrow indicates the direction of crack growth.

Let us consider the following situation. The deformation zone consists of a number of cavitation bands where all the applied strain is concentrated (Fig. 10). In principle, Equation 8 is valid. The relation between the strain rate and the draw speed is now given by

$$v_d = nd_c\dot{\varepsilon} \tag{9}$$

where n is the number of cavitation bands in the deformation zone and d_c is the thickness of the cavitation bands. Now Equation 8 can be rewritten as

$$F_0 = \frac{\lambda}{\rho c_p}\frac{\varepsilon_b}{\dot{\varepsilon} r_c^2} = \frac{\lambda}{\rho c_p}\frac{4n\varepsilon_b}{v_d d_c}$$

where $r_c = \frac{1}{2}d_c$. (10)

When n is taken to be 10, and d_c is 15 μm (both values are estimated from the micrographs), then a draw speed of 1 m s^{-1} will result in $F_0 = 0.98$ and consequently a draw speed of 10 m s^{-1} in $F_0 = 0.1$. This indicates that with the normal impact speed (1 m s^{-1}) the temperature of the material next to the cavitation zones may also rise considerably so that shearbanding becomes possible.

4. Conclusions

When nylon/rubber specimens are fractured under impact conditions, a three-layer structure can be observed. Far away from the fracture surface only cavitation is visible. At a certain point, the previously round cavities become elongated, which indicates that plastic

Figure 10 Schematic representation of a deformation zone with cavitation bands.

deformation has taken place. Directly under the fracture surface is a layer, a few micrometres thick, where practically no cavitation or matrix deformation could be detected. As an explanation for this structure, the hypothesis was put forward that the local temperature rise was high enough to melt the material.

In control experiments it was found that if the deformation and cavitation have disappeared due to thermal effects, the temperature rise had to be high enough to reach the melting temperature.

Calculations suggest that the temperature rise due to plastic deformation alone is not high enough to melt nylon-6. The model, however, is rather sensitive to the actual values of the yield stress and fracture stress and to the shape of the stress–strain curve. Close to the fracture surface, in the high-strain region, chain rupture can result in an extra temperature rise. The combined temperature rise by plastic deformation and chain rupture appears to be high enough to reach the melting point of nylon-6.

The theory of local melting close to the crack plane was supported by SEM studies on specimens fractured under isothermal and adiabatic conditions. Only in specimens fractured under impact conditions could the melt layer be seen. In the low-speed samples, deformed cavities could be seen up to the fracture surface.

When the draw speed is a decade higher than the impact speed the plastic deformation appeared to be concentrated in bands, parallel to the fracture surface. As a possible explanation, the hypothesis was put forward that with very high speeds these thin zones also can deform under adiabatic conditions.

Acknowledgements

We thank Professor dr.ir. L. C. E. Struik for helpful discussions. We are indebted to Akzo, and especially to M. Bosma, for assistance with the high-speed temperature measurements. This work is part of the research programme of the University of Twente and was financially supported by the SON/STW.

References

1. C. B. BUCKNALL, in "Toughened Plastics" (Applied Science, London, 1977).
2. S. CIMMINO, F. COPPOLA, L. D'ORAZIO, R. GRECO, G. MAGLIO, M. MALINCONICO, C. MANCARELLA, E. MARTUSCELLI and G. RAGOSTA, *Polymer* **27** (1986) 1874.
3. F. RAMSTEINER and W. HECKMANN, *Polym. Commun.* **26** (1985) 199.
4. R. J. GAYMANS, R. J. M. BORGGREVE and A. J. OOSTENBRINK, *Makromol. Chem. Makromol. Symp.* **38** (1990) 125.
5. F. SPERONI, E. CASTOLDI, P. FABBRI and T. CASIRAGHI, *J. Mater. Sci.* **24** (1989) 2165.
6. A. J. OOSTENBRINK, K. DIJKSTRA, A. VAN DER WAL and R. J. GAYMANS, P.R.I. Churchill Conference on Deformation and Fracture of Polymers, Cambridge, April 1990, Preprints Paper 50.
7. J. W. BOODE, A. E. H. GAALMAN, A. J. PIJPERS and R. J. M. BORGGREVE, poster presented at the Prague Macromolecular Meeting IUPAC Symposium "Mechansims of Polymer strength and Toughness", Pragve, July 1990.
8. Y. K. GODOVSKY, in "Thermophysical Properties of Polymers" (Springer, Berlin, 1992).
9. Y. K. GODOVSKY, V. S. PAPKOV, A. I. SLUTSKER, E.E. TOMASHEVSKII and G. L. SLONIMSKII, *Solid State Phys.* **13** (1971) 2289.
10. R. P. KAMBOUR and R. E. BARKER, *J. Polym Sci. A-2* **4** (1966) 359.
11. N. LEVY and J. R. RICE, in "Physics of Strength and Plasticity", edited by A. S. Argon (Massachusetts Institute of Technology Press, Cambridge, MA, 1969) p. 252, ref 8.
12. T. FUKUI, Y. KIKUCHI and T. INOUE, *Polymer* **32** (1991) 2367.
13. A. R. POSTEMA, P. SMITH and A. D. ENGLISH, *Polym. Commun.* **31** (1990) 444.
14. K. DIJKSTRA, A. VAN DER WAL and R. J. GAYMANS, *J. Mater. Sci.*, submitted.
15. K. DIJKSTRA, H. H. WEVERS and R. J. GAYMANS, *Polymer* **35** (1994) 323.
16. H. S. CARSLAW and J. C. JAEGER, in "Conduction of Heat in Solids", 2nd Edn (Oxford University Press, 1969) p. 254, ref 8.
17. K. DIJKSTRA, J. TER LAAK and R. J. GAYMANS, *Polymer* **35** (1994) 315.
18. K. DIJKSTRA and G. H. TEN BOLSCHER, *J. Mater. Sci.*, in Press.

Received 25 March
and accepted 17 December 1993